Research Article Received: 2024-02-27, Accepted: 2024-04-09

Bulk heterojunction solar cell using Ru dye attached PCBM

Il-Su Park [a], Jae-Keun Hwang [a], Yongseok Jun [b,*], Donghwan Kim [a,*]

[a] Department of Materials Science and Engineering, Korea University, Seoul, 02841 Republic of Korea

[b] Graduate School of Energy and Environment, Korea University, Seoul, 02841 Republic of Korea

* Corresponding author: yongseok@korea.ac.kr (Y.J.), donghwan@korea.ac.kr (D.K.)

Tel: 82-2-3290-3713

Accepted Manuscript

Abstract

Ru dye (Z-907) is a crucial photosensitizing material in dye-sensitized solar cells (DSSCs). To enhance the utilization of Ru dye's photosensitizing properties in bulk heterojunction solar cells, a method was developed to synthesize phenyl-C61-butyric acid methyl ester (PCBM) nanoparticles that are chemically linked to Ru dye. PCBM contains a methoxy (-OCH_3) group, whereas Ru dye incorporates a carboxyl group (-COOH) within its molecular structure. By exploiting these complementary functional groups, a successful bond between Ru dye and PCBM was established through an anhydride functional group. The coupling of PCBM with Ru dye results in a modification of the energy levels, yielding lower LUMO (3.8 eV) and HOMO (6.1 eV) levels, compared with the LUMO (3.0 eV) and HOMO (5.2 eV) levels of Ru dye alone. This configuration potentially facilitates efficient electron transfer from Ru dye to PCBM, alongside promoting hole transfer from Ru dye to the conducting polymer. Consequently, the bulk heterojunction solar cells incorporating this Ru dye-PCBM

DOI:10.33961/jecst.2024.00262

configuration demonstrate superior performance, with an open circuit voltage (V_{oc}) of 0.62 V, short circuit current (J_{sc}) of 0.63 mA/cm^2, fill factor (FF) of 65.6%, and a photovoltaic conversion efficiency (η) of 0.25%.

Keywords: PCBM, Ru dye(Z-907), Bulk heterojunction solar cells

1. Introduction

Dye-sensitized solar cells (DSSCs) have garnered significant interest due to their straightforward manufacturing process and potential versatility, enabling the integration of aesthetically appealing designs in various applications [1-6]. Despite the diverse research avenues within this field, the direct application of efficient Ru dyes in the primary absorption layer, particularly within heterojunction solar cells, has remained limited [7-10]. Ru dyes are extensively utilized as photosensitizers in DSSCs, where they are typically coated onto TiO_2 surfaces using carboxylic functional groups for attachment [11-13]. These groups are crucial for connecting Ru dyes with conventional materials widely used in bulk heterojunction organic solar cells, notably including Fullerene-type compounds such as C60, PCBM, and CNTs [14-16].

Considering dyes as primary components, the integration of electron acceptors becomes essential when combining Ru dyes with fullerene-type materials. Although C60 exhibits stronger electron-accepting properties than PCBM, the latter material's remarkable solubility in organic solvents, such as toluene, and superior electron mobility relative to C60, render it more effective in bulk heterojunction solar cells [17, 18]. Therefore, substituting PCBM with C60 in organic heterojunction solar cells represents a significant challenge.

This experimental study introduced Z-907, commonly referred to as black dye,

DOI:10.33961/jecst.2024.00262

Accepted Manuscript

characterized by an extended alkyl group within the molecular structure of the Ru dye. The presence of this elongated alkyl group renders Z-907 a hydrophobic photosensitizer in DSSCs, countering the adverse effects of hydrophilic liquid electrolytes [19, 20]. Z907 represents a paradigmatic advancement among the N-series dyes, extensively scrutinized for their efficacy in DSSCs. The robust investigation into Ru-based dyes for DSSCs continues to be a pivotal research trajectory. The foundational functionalities and fundamental principles have been elucidated by Najm et al., while the expansive spectrum of applications facilitated by amalgamating Ru-based dyes remains an important research theme in the realm of DSSCs [2, 12, 21, 22]. Despite being acknowledged as potent materials for energy harvesting, Ru-based dyes have yet to find direct application in organic solar cells. Limited instances, such as the adsorption of Ru-dyes onto carbonaceous materials for organic solar cell applications, have been reported [23]. While reminiscent of our approach, these applications lack consideration of chemical interactions.

We posited that, by attaching Ru dye to the surface of PCBM for the first time, we could enhance electron generation, thus increasing the photocurrent in solar cells compared with those without Ru dye. To explore this hypothesis, we synthesized a novel material known as Ru dye-PCBM, leveraging the methoxy group found in PCBM and the carboxyl group present in Z-907. A notable characteristic of Ru dye-PCBM is its excellent solubility in hydrophobic solvents, such as chloroform and 2-chlorobenzene, facilitating its integration into the blend layer of poly-3-octylthiophene (P3OT) polymer for use in our solar cells. Following these steps, we fabricated bulk heterojunction solar cells incorporating the blend layer composed of Ru dye-PCBM and P3OT, enabling us to examine the effects of Ru dye-PCBM on the photovoltaic performance of the solar cells.

2. Experiment

DOI:10.33961/jecst.2024.00262

Accepted Manuscript

In our experimental procedure, we utilized phenyl-C61-butyric acid methyl ester (PCBM) and Ru dye (Z-907, Solaronix) to synthesize a composite material, termed Ru dye-PCBM, through a chemical attachment of Ru dye to PCBM. To achieve an optimal 1:1 molar ratio between PCBM and Ru dye, we combined 0.1 g of Ru dye with 0.1 g of PCBM in a dimethylformamide (DMF) solvent. The mixture was subjected to reflux at 60 ℃ for a period of one day. Following this, the DMF solvent was removed via vacuum aspiration with several washing, and the product was dried in a vacuum oven set at 25 ℃. The synthetic process of chemically attaching Ru dye to PCBM is illustrated in Figure 1.

A glass/ITO substrate (2.5 cm x 1.5 cm) is prepared for thin film deposition. The substrate is loaded onto a spin coater, and 100 μl of PEDOT:PSS solution is dripped onto it before spinning at 3000 rpm. After spinning, it is dried using a dryer for 30 seconds. Subsequently, 100 μl of each of the three prepared solutions (Ru dye, PCBM, or Ru dye with PCBM) are dripped onto the substrate, followed by spinning at 3000 rpm and drying with a dryer for 30 seconds. The samples are then heat-treated at 100 ℃ for 30 minutes. Finally, Al is deposited through an evaporator to form the electrode.

For structural characterization of the Ru dye-PCBM composite, we employed several analytical techniques, including infrared (IR) spectroscopy, ultraviolet-visible (UV-Vis) spectroscopy, transmission electron microscopy (TEM), and energy dispersive X-ray (EDX) analysis. To evaluate the photovoltaic performance of bulk heterojunction solar cells incorporating Ru dye-PCBM, we utilized J-V curves. These curves are instrumental in offering detailed information on the efficiency and operational capabilities of our solar cell system, highlighting the potential impact of Ru dye-PCBM on enhancing solar cell performance.

Accepted Manuscript

DOI:10.33961/jecst.2024.00262

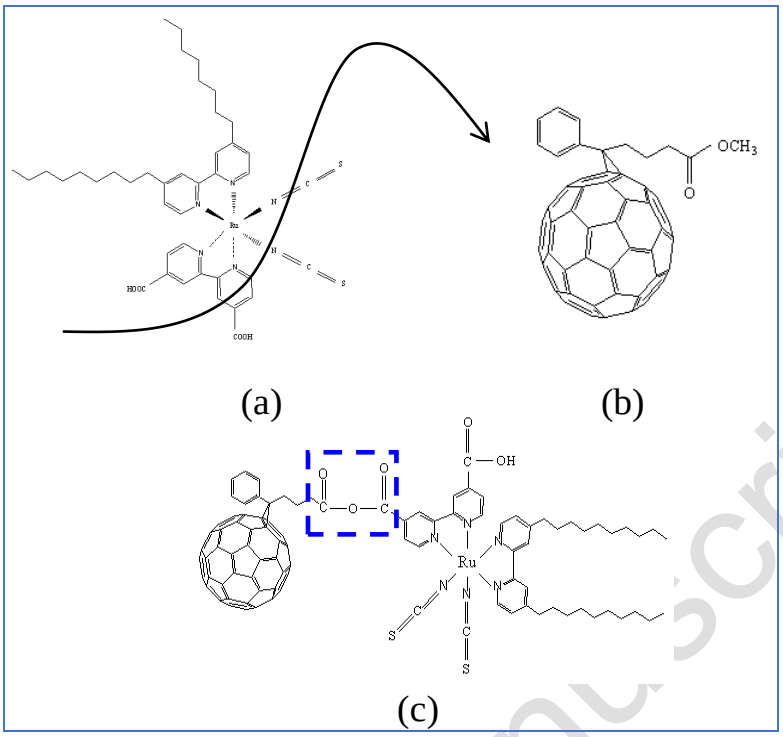

Figure 1. Synthetic mechanism of Ru dye-PCBM particle.

(a) Ru dye (Z-907, Solaronix), (b) PCBM, (c) Ru dye attached with PCBM (Ru dye-PCBM). rectangle region: anhydride bonding

3. Results and Discussions

To evaluate the interaction between fullerene and Z907, IR spectroscopy was utilized. This analytical technique enabled the identification of effective bonding between Z907 and PCBM, as depicted in Figure 1c. The analysis yielded specific spectral peaks, detailed in Figure 2, which are indicative of the chemical interactions within the composite material. Notably, anhydride bonds were characterized by distinctive spectral features, including two prominent doublet peaks at 1613 cm^{-1} and 1733 cm^{-1}, attributed to the C=O stretching mode. Normally, carboxylic acid peak gives a strong C=O stretching peak. Additionally, peaks at 1231 cm^{-1} and 1255 cm^{-1} were observed, corresponding to the C-O stretching mode. The presence of the N=C=S group in the Ru dye was confirmed by a distinct peak at 2096 cm^{-1}. These spectral signatures provide crucial insights into the chemical bonding and interactions present in our

Accepted Manuscript

DOI:10.33961/jecst.2024.00262

experimental system, highlighting the successful integration of Z907 and PCBM.

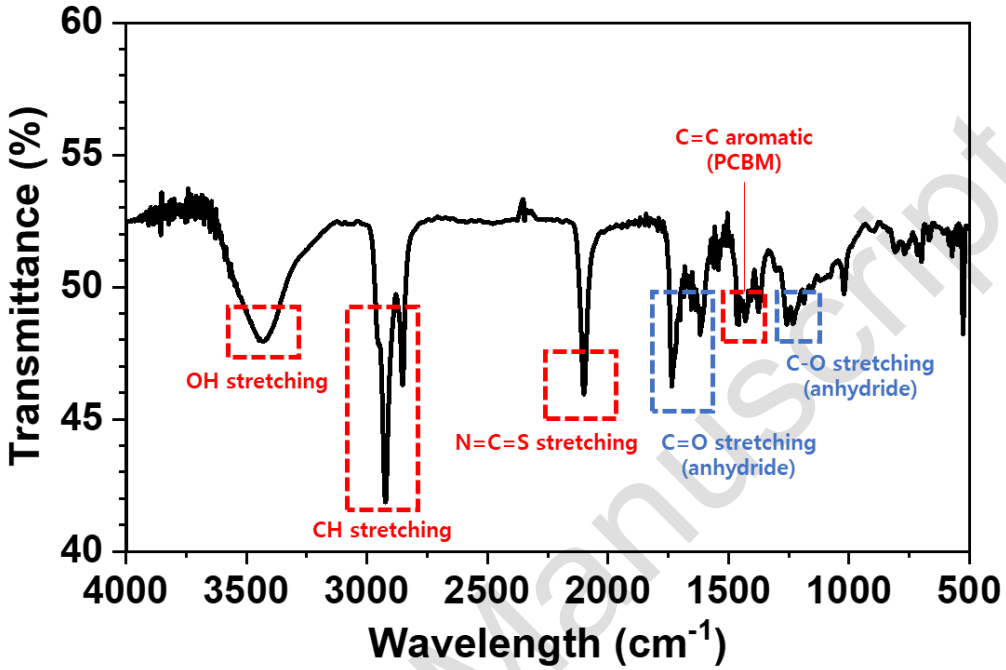

Figure 2. IR spectra of Ru-dye-PCBM particles.

Moreover, UV-Vis absorptive spectroscopy was employed to examine the interaction between Ru dye and PCBM. As illustrated in Figure 3, Ru dye exhibits two prominent absorption peaks at wavelengths of λ = 450 nm and λ = 570 nm, whereas PCBM presents a distinct peak at λ = 430 nm. Notably, the UV-Vis absorption spectrum of the Ru dye-PCBM composite displays three peaks at λ = 430 nm, λ = 450 nm, and λ = 570 nm, resembling the individual absorption characteristics of Ru dye and PCBM. This analysis robustly corroborates the existence of anhydride bonding between Ru dye and PCBM, thus reinforcing the findings obtained from IR spectroscopy and providing a comprehensive understanding of the chemical interactions within the composite material.

Accepted Manuscript

DOI:10.33961/jecst.2024.00262

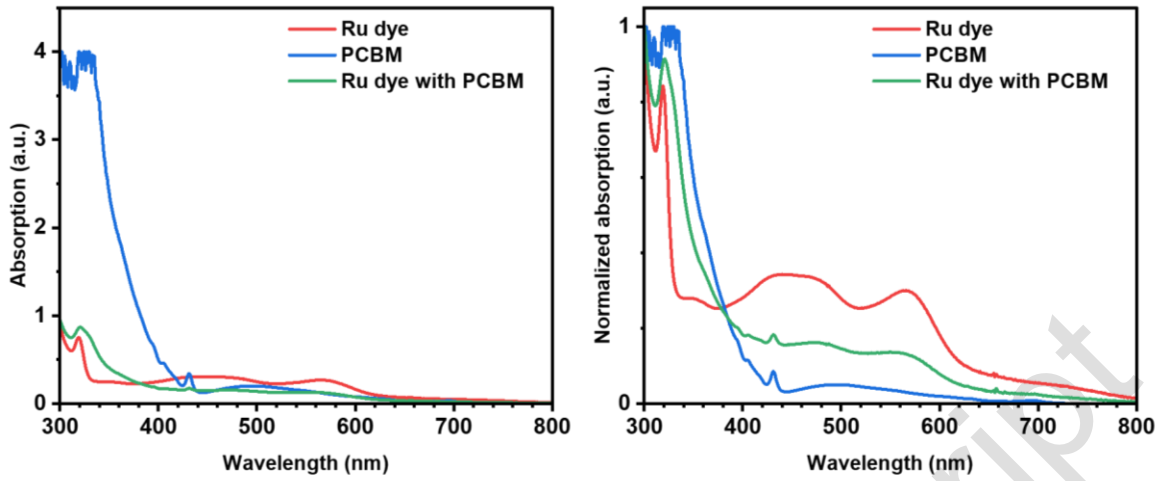

Figure 3. UV-Vis absorptive spectra of Ru dye-PCBM particles.

The analysis of Ru dye-PCBM particles was conducted via TEM. The TEM images, as shown in Figure 4, revealed an interesting phenomenon where PCBM particles appear to aggregate due to van der Waals forces. While the TEM imagery of Ru dye-PCBM does not distinctly differentiate between Ru dye and PCBM, subsequent EDX analysis of the red section highlighted the presence of Ru dye particles on the surface of Ru dye-PCBM particles.

This observation was further supported by the detection of specific elements, particularly Ru and S, in the EDX spectra. These elements serve as markers for the presence of Ru dye, attributed to the two N=C=S ligand groups inherent in Z-907 [24, 25]. Thus, the combination of TEM and EDX analyses effectively confirms the successful bonding between Ru dye and PCBM, improving the understanding of the chemical composition and interaction within the composite material.

Accepted Manuscript

DOI:10.33961/jecst.2024.00262

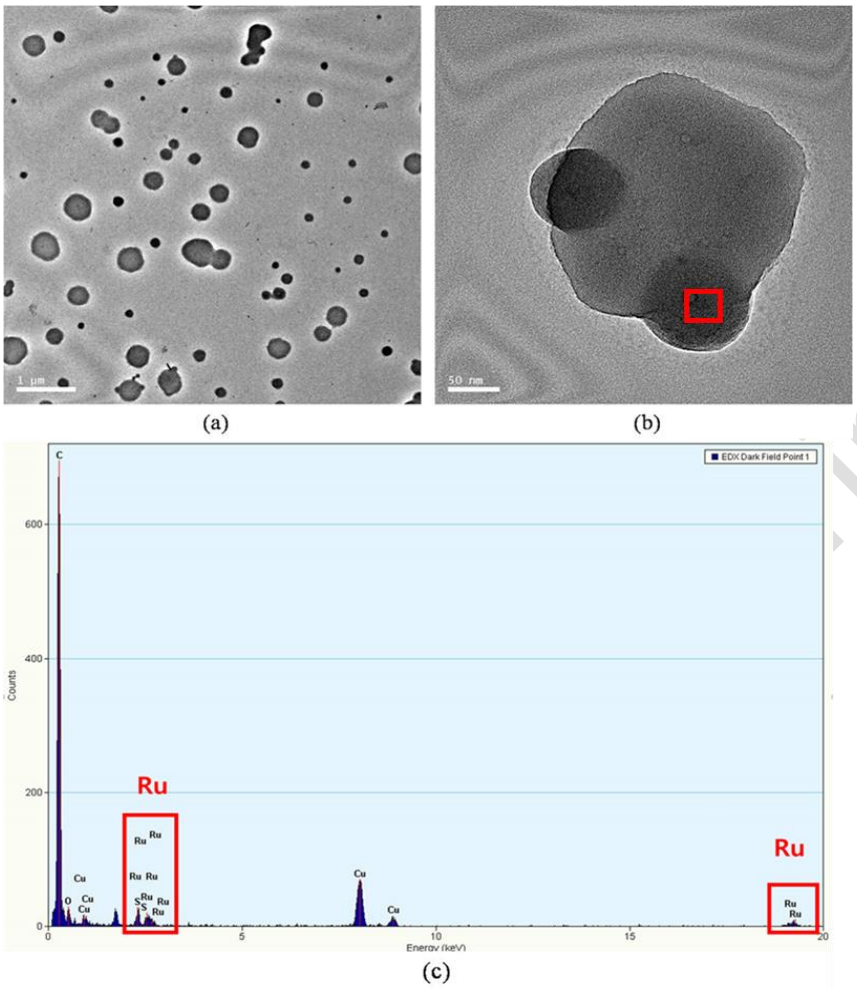

Figure 4. TEM data (a, b) and EDX (c) of Ru dye-PCBM particle (red region in (b)).

Ru dye serves as a photosensitizer and electron donor, unlike PCBM, which acts as an electron acceptor. Within the Ru dye-PCBM system, the energy levels demonstrate a notable difference, with PCBM presenting lower LUMO (3.8 eV) and HOMO (6.1 eV) levels compared with those of Ru dye, which are LUMO: 3.0 eV and HOMO: 5.2 eV [26]. This variation in energy levels enables Ru dye to absorb light within the wavelength range of λ = 450–570 nm, facilitating the generation of excitons within the Ru dye-PCBM particle.

Upon the creation of these excitons at the interface between Ru dye and the conducting polymer, PCBM's role as an efficient electron acceptor becomes crucial. It effectively promotes the transfer of photoelectrons to the metal layer, indicating facile electron transfer

DOI:10.33961/jecst.2024.00262

from Ru dye to PCBM. This process is accompanied by the movement of holes from Ru dye to the conducting polymer, further illustrating the synergistic interaction within the Ru dye–PCBM composite, as depicted in Figure 5.

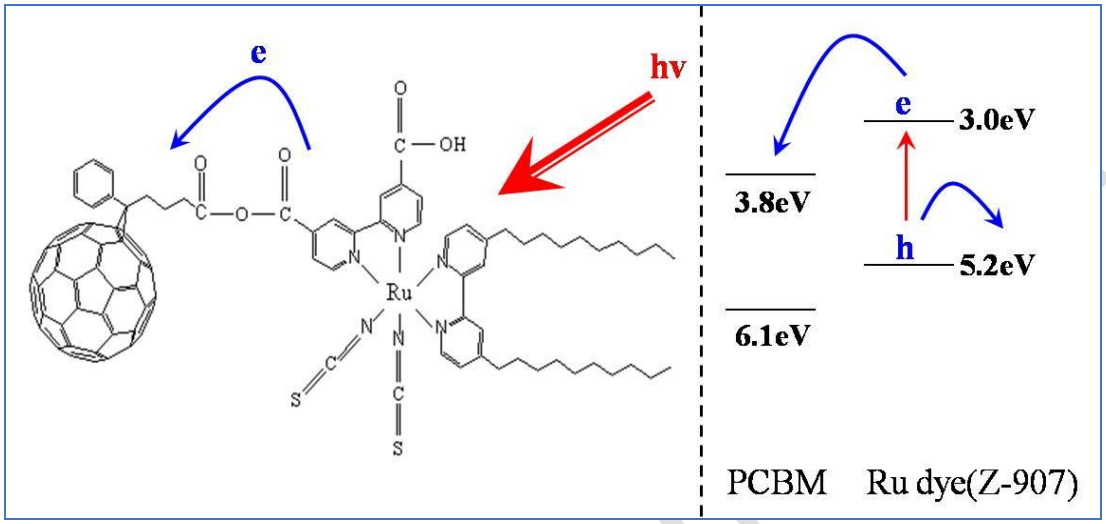

Figure 5. Schematic of charge transfer in Ru dye-PCBM particles.

Figure 6 illustrates the composition of bulk heterojunction solar cells, encompassing layers of indium tin oxide (ITO) glass, PEDOT:PSS (40 nm), a blended active layer comprising Ru dye-PCBM particles and P3OT (Poly-3-octylthiophene), culminating in a terminal layer of Al measuring 100 nm. The process of hole transfer within these cells primarily operates through diffusion, attributed to the analogous HOMO energy levels of Ru dye, P3OT, and PEDOT:PSS. This similarity facilitates the potential recombination of holes with electrons, which in turn yields a modest current output for the solar cells. HOMO levels of Ru dyes, P3OT, and PEDOT:PSS are very close to each other with the value of 5.2 eV, and this matching may result in no resistance or very small amount of resistance in the device. If the hole passing may need an extra activation energy, this may cause small voltage drop in Voc.

Accepted Manuscript

DOI:10.33961/jecst.2024.00262

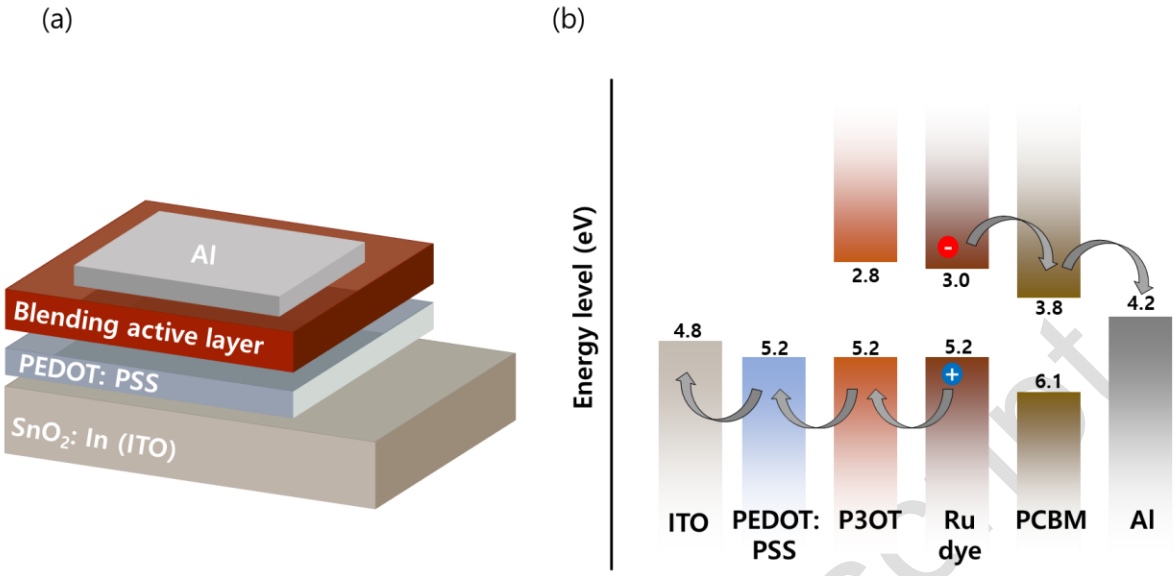

Figure 6. (a) Structure and (b) energy level of bulk heterojunction solar cells using Ru dye-PCBM particles.

PCBM particles play a crucial role in enhancing the photovoltaic properties of Ru dye-PCBM particles. As depicted in Figure 7, these particles are uniformly dispersed throughout the P3OT layer without noticeable aggregated spots.

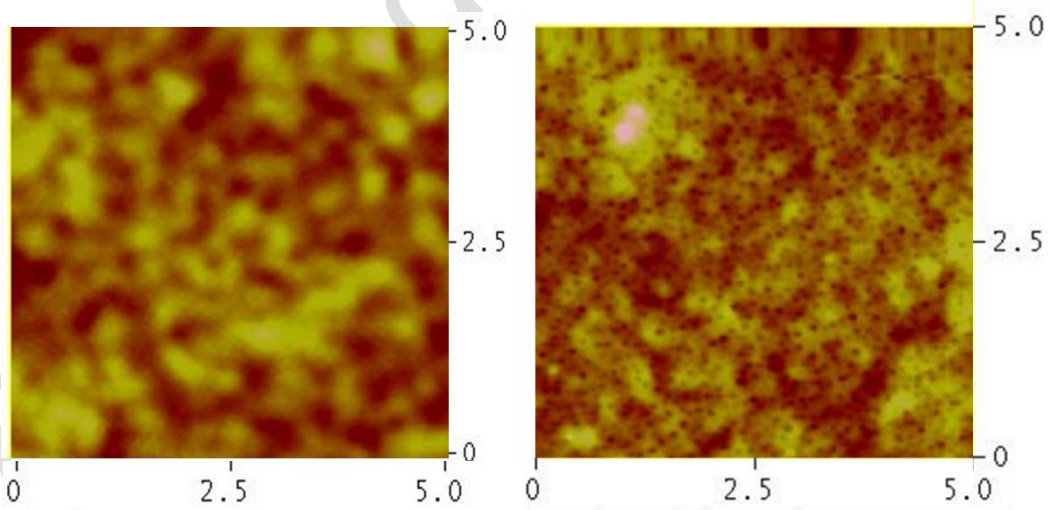

(a) (b)

Figure 7. AFM data of (a) P3OT film, (b) Ru dye-PCBM:P3OT blending film on ITO glass (x-y scale : μm, z scale : nm upto 50 nm).

Figure 8 and Table 1 present an analysis of the photovoltaic performance of bulk

DOI:10.33961/jecst.2024.00262

heterojunction-type solar cells incorporating Ru dye, PCBM, and Ru dye-PCBM particles. To evaluate the influence of Ru dye on the PCBM surface within both Ru dye and Ru dye-PCBM blending solutions, an equivalent quantity of PCBM particles was employed. The comparison of electron generation between PCBM and Ru dye particles elucidates the beneficial effect of Ru dye on the photovoltaic attributes of heterojunction solar cells, primarily attributed to Ru dye's ability to generate excitons, akin to P3OT. The incorporation of Ru dye-PCBM particles results in a substantial 50% increase in the solar cell's short-circuit current (J_{sc}) in comparison to cells with only PCBM particles, although the total cell efficiency remains modest.

Notably, Ru dye particles alone do not seem to support electron transfer through a hopping process, unlike PCBM particles, as indicated by the absence of J_{sc} and open-circuit voltage (V_{oc}) improvements in Figure 8. Nonetheless, the utilization of Ru dye-PCBM particles enhances the solar cells' fill factor relative to cells with only PCBM particles. This increase in fill factor may be attributed to a more effective interface established between Ru dye-PCBM particles and P3OT, though the specific mechanisms underlying this enhanced interface are yet to be fully understood. A plausible rationale is that Ru dye-PCBM particles more efficiently facilitate exciton separation than PCBM alone, as PCBM tends to attract electrons generated from the absorption of light by Ru dye.

The bulk heterojunction solar cells incorporating Ru dye-PCBM particles demonstrate notable performance metrics: V_{oc} = 0.62 V, J_{sc} = 0.63 mA/cm^2, FF = 65.6 %, and η = 0.25%. This marks a significant enhancement in photovoltaic efficiency relative to solar cells employing PCBM alone, effectively doubling the overall efficiency. Hence, Ru dye particles contribute positively to the photovoltaic properties of bulk heterojunction solar cells by enhancing electron generation alongside P3OT.

Accepted Manuscript

DOI:10.33961/jecst.2024.00262

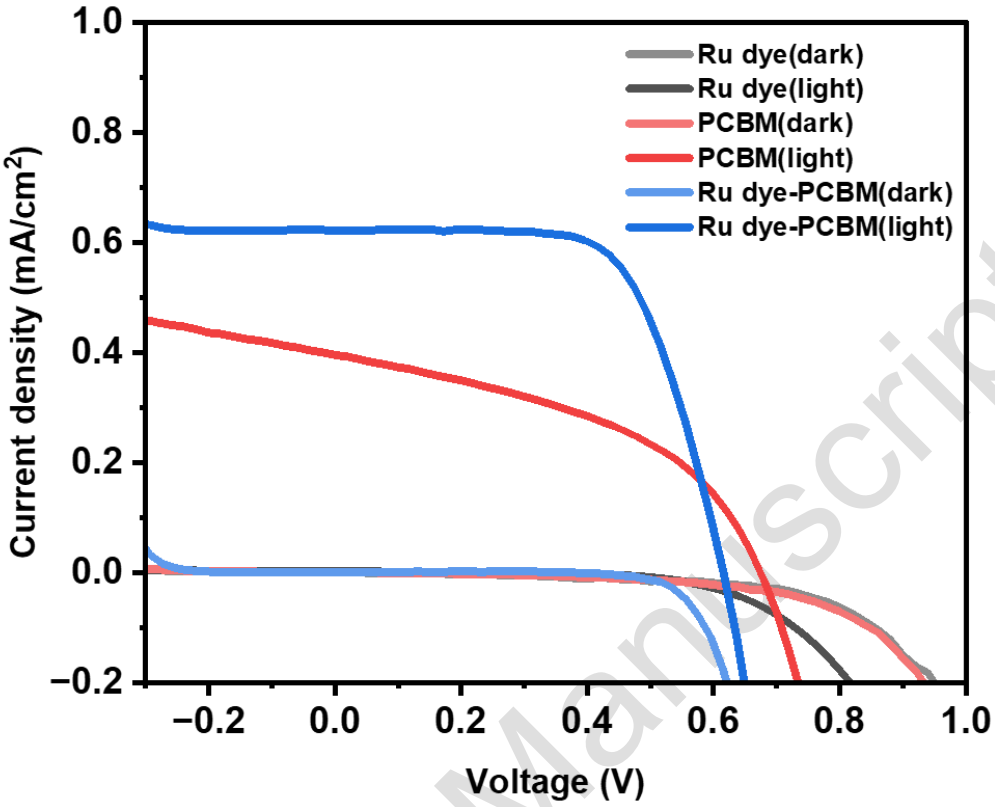

Figure 8. JV curves of heterojunction solar cells using blending layer.

Table 1. Comparison of the device performance of heterojunction solar cells using blending layer

	V_{oc} (V)	J_{sc} (mA/cm^2)	PCE (%)	FF (%)
Ru dye	0	0	0	0
PCBM	0.67	0.40	0.12	44.8
PCBM with Ru dye	0.60	0.62	0.25	67.2

4. Conclusion

DOI:10.33961/jecst.2024.00262

Accepted Manuscript

The incorporation of Ru-dye-linked particles in DSSCs has emerged as an effective strategy for electron generation via light absorption. Our research endeavors have culminated in the successful synthesis of Ru dye-PCBM via anhydride bonding, targeting its application in bulk heterojunction solar cells. The introduction of Ru dye-PCBM particles into these cells has markedly augmented photovoltaic efficiency, achieving an enhancement that is nearly double that observed with the sole use of PCBM particles. This significant improvement is ascribed to the dual role of Ru dye: it not only facilitates electron generation by enabling exciton separation at the interface but also promotes the attraction of electrons from excitons generated during light absorption.

Acknowledgements

This work was supported by "Human Resources Program in Energy Technology" of the Korea Institute of Energy Technology Evaluation and Planning (KETEP), granted financial resource from the Ministry of Trade, Industry & Energy, Republic of Korea. (No. 20204010600470 & No. 20213091010020)

Reference

1. Oregan, B.; Gratzel, M., A Low-Cost, High-Efficiency Solar-Cell Based on Dye-Sensitized Colloidal Tio2 Films. Nature 1991, 353, (6346), 737-740.
2. Balasingam, S. K.; Lee, M.; Kang, M. G.; Jun, Y., Improvement of dye-sensitized solar cells toward the broader light harvesting of the solar spectrum. Chem Commun 2013, 49, (15), 1471-1487.
3. Kim, J.; Lim, J.; Kim, M.; Lee, H. S.; Jun, Y.; Kim, D., Fabrication of Carbon-Coated Silicon Nanowires and Their Application in Dye-Sensitized Solar Cells. Acs Appl

DOI:10.33961/jecst.2024.00262

Accepted Manuscript

Mater Inter 2014, 6, (21), 18788-18794.

4. Rahman, M. M.; Kang, H. C.; Yoo, K.; Lee, J. J., Low-Temperature Chemical Sintered TiO2 Photoanodes Based on a Binary Liquid Mixture for Flexible Dye-Sensitized Solar Cells. J Electrochem Sci Te 2022, 13, (4), 453-461.
5. Ko, Y.; Choi, W.; Kim, Y.; Lee, C.; Jun, Y.; Kim, J., Synthesis of CoSe/RGO Composites and Its Application as a Counter Electrode for Dye-Sensitized Solar Cells. J Electrochem Sci Te 2019, 10, (3), 313-320.
6. Nam, H.; Ko, Y.; Kunnan, S. C.; Choi, N. S.; Jun, Y., Synthesis and Applications of Dicationic Iodide Materials for Dye-Sensitized Solar Cells. J Electrochem Sci Te 2019, 10, (2), 214-222.
7. Prakash, P.; Janarthanan, B., Review on the progress of light harvesting natural pigments as DSSC sensitizers with high potency. Inorg Chem Commun 2023, 152.
8. Gao, H. Z.; Yu, R. N.; Ma, Z. W.; Gong, Y. S.; Zhao, B. A.; Lv, Q. L.; Tan, Z. A., Recent advances of organometallic complexes in emerging photovoltaics. J Polym Sci 2022, 60, (6), 865-916.
9. Wang, B. N.; Li, N.; Yang, L.; Dall'Agnese, C.; Jena, A. K.; Miyasaka, T.; Wang, X. F., Organic Dye/CsAgBiBr Double Perovskite Heterojunction Solar Cells. J Am Chem Soc 2021, 143, (36), 14877-14883.
10. Grätzel, M., Dye-sensitized solid-state heterojunction solar cells. Mrs Bull 2005, 30, (1), 23-27.
11. Joshy, D.; Narendranath, S. B.; Ismail, Y. A.; Periyat, P., Recent progress in one dimensional TiO nanomaterials as photoanodes in dye-sensitized solar cells. Nanoscale Adv 2022, 4, (24), 5202-5232.
12. Najm, A. S.; Alwash, S. A.; Sulaiman, N. H.; Chowdhury, M. S.; Techato, K., N719 dye as a sensitizer for dye-sensitized solar cells (DSSCs): A review of its functions

DOI:10.33961/jecst.2024.00262

Accepted Manuscript

and certain rudimentary principles. Environ Prog Sustain 2023, 42, (1).

13. Tomar, N.; Agrawal, A.; Dhaka, V. S.; Surolia, P. K., Ruthenium complexes based dye sensitized solar cells: Fundamentals and research trends. Sol Energy 2020, 207, 59-76.

14. Yu, G.; Gao, J.; Hummelen, J. C.; Wudl, F.; Heeger, A. J., Polymer Photovoltaic Cells - Enhanced Efficiencies Via a Network of Internal Donor-Acceptor Heterojunctions. Science 1995, 270, (5243), 1789-1791.

15. Conturbia, G.; Vinhas, R. D. G.; Landers, R.; Valente, G. M. S.; Baranauskas, V.; Nogueira, A. F., Single-Wall Carbon Nanotubes Chemically Modified with Cysteamine and Their Application in Polymer Solar Cells: Influence of the Chemical Modification on Device Performance. J Nanosci Nanotechno 2009, 9, (10), 5850-5859.

16. Backer, S. A.; Sivula, K.; Kavulak, D. F.; Fréchet, J. M. J., High efficiency organic photovoltaics incorporating a new family of soluble fullerene derivatives. Chem Mater 2007, 19, (12), 2927-2929.

17. Li, G.; Shrotriya, V.; Huang, J. S.; Yao, Y.; Moriarty, T.; Emery, K.; Yang, Y., High-efficiency solution processable polymer photovoltaic cells by self-organization of polymer blends. Nature materials 2005, 4, (11), 864-868.

18. Reyes-Reyes, M.; Kim, K.; Carroll, D. L., High-efficiency photovoltaic devices based on annealed poly(3-hexylthiophene) and 1-(3-methoxycarbonyl)-propyl-1-phenyl-(6,6)C blends -: art. no. 083506. Appl Phys Lett 2005, 87, (8).

19. Klein, C.; Nazeeruddin, K.; Di Censo, D.; Liska, P.; Grätzel, M., Amphiphilic ruthenium sensitizers and their applications in dye-sensitized solar cells. Inorg Chem 2004, 43, (14), 4216-4226.

20. Yanagida, S.; Yu, Y. H.; Manseki, K., Iodine/Iodide-Free Dye-Sensitized Solar Cells. Accounts Chem Res 2009, 42, (11), 1827-1838.

DOI:10.33961/jecst.2024.00262

Accepted Manuscript

21. Mede, T.; Jäger, M.; Schubert, U. S., "Chemistry-on-the-complex": functional Ru polypyridyl-type sensitizers as divergent building blocks. Chemical Society reviews 2018, 47, (20), 7577-7627.

22. Shalini, S.; Balasundaraprabhu, R.; Kumar, T. S.; Prabavathy, N.; Senthilarasu, S.; Prasanna, S., Status and outlook of sensitizers/dyes used in dye sensitized solar cells (DSSC): a review. Int J Energ Res 2016, 40, (10), 1303-1320.

23. Lee, T. Y.; Yoo, J. B., Adsorption characteristics of Ru(II) dye on carbon nanotubes for organic solar cell. Diam Relat Mater 2005, 14, (11-12), 1888-1890.

24. Yanagida, S.; Senadeera, G. K. R.; Nakamura, K.; Kitamura, T.; Wada, Y., Polythiophene-sensitized TiO solar cells. J Photoch Photobio A 2004, 166, (1-3), 75-80.

25. Jang, S. R.; Vittal, R.; Kim, K. J., Incorporation of functionalized single-wall carbon nanotubes in dye-sensitized TiO solar cells. Langmuir 2004, 20, (22), 9807-9810.

26. Bisquert, J.; Grätzel, M.; Wang, Q.; Fabregat-Santiago, F., Three-channel transmission line impedance model for mesoscopic oxide electrodes functionalized with a conductive coating. J Phys Chem B 2006, 110, (23), 11284-11290.

Figure Legends:

Figure 9. Synthetic mechanism of Ru dye-PCBM particle. (a) Ru dye (Z-907, Solaronix), (b) PCBM, (c) Ru dye attached with PCBM (Ru dye-PCBM). rectangle region: anhydride bonding

Figure 10. IR spectra of Ru-dye-PCBM particles.

Figure 11. UV-Vis absorptive spectra of Ru dye-PCBM particles.

Figure 12. TEM data (a, b) and EDX (c) of Ru dye-PCBM particle (red region in (b)).

Figure 13. Schematic of charge transfer in Ru dye-PCBM particles.

DOI:10.33961/jecst.2024.00262

Accepted Manuscript

Figure 14. (a) Structure (a) and energy level (b) of bulk heterojunction solar cells using Ru dye-PCBM particles.

Figure 15. AFM data of (a) P3OT film, (b) Ru dye-PCBM:P3OT blending film on ITO glass

(Scale : ㎛).

Figure 16. JV curves of heterojunction solar cells using blending layer.

Accepted Manuscript

DOI:10.33961/jecst.2024.00262